

Relationships among Resonant Frequency Changes on a Coated Quartz Crystal Microbalance, Thickness Changes, and Resistance Responses of Polymer–Carbon Black Composite Chemiresistors

Erik J. Severin and Nathan S. Lewis*

Division of Chemistry and Chemical Engineering, California Institute of Technology, Pasadena, California 91125

The relationships among frequency changes on a film-coated quartz crystal microbalance, thickness changes, and dc resistance changes have been investigated for carbon black–insulating polymer composite vapor detectors. Quartz crystal microbalance (QCM) measurements and ellipsometry measurements have been performed simultaneously on polymer films that do not contain carbon black filler to relate the QCM frequency change and the ellipsometrically determined thickness change to the analyte concentration in the vapor phase. In addition, quartz crystal microbalance measurements and dc resistance measurements on carbon black composites of these same polymers have been performed simultaneously to relate the QCM frequency change and dc electrical resistance response to the analyte concentration in the vapor phase. The data indicate that the dc resistance change is directly relatable to the thickness change of the polymers and that a variety of analytes that produce a given thickness change produce a constant resistance change for each member of the test set of polymers investigated in this work.

Carbon black–insulating organic polymer composite films have been employed previously as components of an array of vapor detectors for use in an “electronic nose”.¹ In this approach, the response of an array of broadly cross-responsive vapor detectors is analyzed using standard chemometric methods to yield diagnostic patterns that allow classification and quantification of analytes in the vapor phase. Arrays of such detectors have been shown to be highly discriminating, even between very structurally similar analytes, and have also been shown for many test vapors to exhibit a linear steady-state dc resistance response to analyte concentration. Thus, under these conditions, the pattern type allows identification of the vapor and the steady-state pattern height allows quantification of the analyte of concern.^{1–3}

The resistance response of such composites can, in general, be understood by percolation theory, which relates the resistance

response of a composite consisting of an insulating polymer filled with regions of an electrical conductor to the change in volume fraction of the conducting (filler) phase of the composite.^{4–7} The goal of the present work was to elucidate the factors that control the resistance change of such films in response to a change in the concentration of a vapor that is exposed to the detector. In polymer-coated quartz crystal microbalances, the frequency change of the detector is primarily determined by the change in the mass of analyte sorbed into the polymer film for relatively small frequency shifts and/or small changes in the viscoelastic properties of the film.^{8a,b} Polymer-coated surface acoustic wave devices, utilize changes in sorbed mass and modulus of the polymer film to produce the detected signal.^{8c} The hypothesis that was challenged in this work is that the volume change, and thus the fractional swelling, of the polymer film upon exposure to a test vapor is the key variable that determines the change in dc electrical resistance of the carbon black–polymer composite detectors.

To test this hypothesis, we performed measurements to determine the resonant frequency changes on a film-coated quartz crystal microbalance (QCM), the thickness changes, and the resistance changes of various composite and noncomposite polymer films exposed to a variety of test organic vapors. The resonant frequency changes and the dc electrical resistance changes of a set of carbon black–organic polymer composite films were determined on a QCM. QCM measurements and thickness measurements using fixed-wavelength ellipsometry methods were then performed on clear (non-carbon-black-filled) films formed from the same polymers. Relationships between the two sets of measurements were facilitated because at a given analyte concentration in the vapor phase, the measured QCM resonant frequency changes were very similar for polymers that did, and did not, contain the carbon black filler material.

- (1) Lonergan, M. C.; Severin, E. J.; Doleman, B. J.; Beaver, S. A.; Grubbs, R. H.; Lewis, N. S. *Chem. Mater.* **1996**, *8*, 2298.
- (2) Freund, M. S.; Lewis, N. S. *Proc. Natl. Acad. Sci. U.S.A.* **1995**, *92*, 2652–2656.
- (3) Doleman, B. J.; Lonergan, M. C.; Severin, E. J.; Vaid, T. P.; Lewis, N. S. *Anal. Chem.* **1998**, *70*, 4177–4190.

- (4) Anderson, J. E.; Adams, K. M.; Troyk, P. R. *J. Non-Cryst. Sol.* **1991**, *131*, 587–592.
- (5) Ast, D. G. *Phys. Rev. Lett.* **1974**, *33*, 1042–1045.
- (6) Godovski, D. Y.; Koltypin, E. A.; Volkov, A. V.; Moskvina, M. A. *Analyst* **1993**, *118*, 997–999.
- (7) Kirkpatrick, S. *Rev. Mod. Phys.* **1973**, *45*, 574–588.
- (8) (a) Lu, C. In *Applications of Piezoelectric Quartz Crystal Microbalances*; Lu, C. C., Ed.; Elsevier: New York, 1984; Vol. 7, pp 19–61. (b) Buttry, D. A. In *Electroanalytical Chemistry: A Series of Advances*; Bard, A. J., Ed.; Marcel Dekker: New York, 1991; Vol. 17, pp 1–85. (c) Grate, J. W.; Klusty, M.; McGill, R. A.; Abraham, M. H.; Whiting, G.; Andonian-Haftvan, J. *Anal. Chem.* **1992**, *64*, 610–624.

Table 1: Correlation Coefficients, Slopes, Intercepts, Intercept Errors, and Slope Errors for the Eight Solvents and Two Polymer Systems Used in This Work^a

PCL composite film	Δf^*_{max} vs P/P°					$\Delta R_{\text{max}}/R_b$ vs P/P°					$\Delta R_{\text{max}}/R_b$ vs Δf^*_{max}				
	R^2	intcpt	slp	intcpt err	slp err	R^2	intcpt	slp	intcpt err	slp err	R^2	intcpt	slp	intcpt err	slp err
hexane	0.9997	0.00	3.64	0.006	0.034	0.9989	0.00	17.99	0.066	0.344	0.9991	0.01	11.61	0.059	0.197
2-propanol	0.9934	0.02	3.44	0.028	0.161	0.9933	0.04	15.93	0.130	0.754	0.9999	-0.05	10.88	0.018	0.070
benzene	0.9976	0.38	15.18	0.078	0.429	0.9968	0.40	76.98	0.456	2.520	0.9987	-1.52	11.89	0.330	0.252
dichloromethane	0.9998	-0.06	20.91	0.046	0.159	0.9993	-0.60	71.15	0.317	1.099	0.9987	-0.38	7.98	0.420	0.165
chloroform	0.9998	0.19	46.08	0.078	0.384	0.9988	0.21	145.40	0.604	2.962	0.9984	-0.38	7.40	0.694	0.170
hexafluorobenzene	0.9937	0.54	13.65	0.113	0.628	0.9969	0.78	35.03	0.203	1.124	0.9987	-0.58	5.99	0.158	0.127
dibromomethane	0.9974	-0.04	55.04	0.280	1.620	0.9960	-1.31	105.29	0.668	3.861	0.9991	-1.23	4.49	0.319	0.079
bromoform	0.9989	0.41	76.41	0.245	1.481	0.9982	-1.16	137.74	0.558	3.375	0.9983	-1.88	4.22	0.558	0.101

PCL clear film	Δf^*_{max} vs P/P°					$\Delta h_{\text{max}}/h_b$ vs P/P°					$\Delta h_{\text{max}}/h_b$ vs Δf^*_{max}				
	R^2	intcpt	slp	intcpt err	slp err	R^2	intcpt	slp	intcpt err	slp err	R^2	intcpt	slp	intcpt err	slp err
hexane	0.9981	0.01	1.84	0.012	0.031	0.9909	0.02	0.55	0.008	0.021	0.9926	0.01	0.70	0.007	0.024
2-propanol	0.9971	-0.02	3.67	0.040	0.081	0.9932	-0.03	1.10	0.019	0.037	0.9987	-0.02	0.70	0.008	0.010
benzene	0.9956	0.18	10.40	0.039	0.273	0.9928	0.05	3.02	0.015	0.101	0.9967	0.00	0.68	0.011	0.015
dichloromethane	0.9992	-0.13	17.70	0.041	0.192	0.9963	-0.03	3.65	0.018	0.084	0.9950	0.00	0.48	0.020	0.013
chloroform	0.9984	0.00	42.96	0.121	0.685	0.9967	-0.03	8.43	0.033	0.189	0.9984	-0.03	0.46	0.023	0.007
hexafluorobenzene	0.9973	0.15	9.20	0.097	0.175	0.9984	-0.02	1.43	0.012	0.021	0.9985	-0.04	0.36	0.011	0.005
dibromomethane	0.9980	0.56	44.16	0.154	0.667	0.9989	-0.01	5.88	0.015	0.064	0.9993	-0.08	0.31	0.012	0.003
bromoform	0.9977	-0.05	66.71	0.187	1.256	0.9977	-0.05	7.94	0.022	0.151	0.9981	-0.04	0.28	0.020	0.005

PEO composite film	Δf^*_{max} vs P/P°					$\Delta R_{\text{max}}/R_b$ vs P/P°					$\Delta R_{\text{max}}/R_b$ vs Δf^*_{max}				
	R^2	intcpt	slp	intcpt err	slp err	R^2	intcpt	slp	intcpt err	slp err	R^2	intcpt	slp	intcpt err	slp err
hexane	0.9985	0.01	0.97	0.003	0.014	0.9990	-0.02	9.89	0.025	0.117	0.9970	-0.06	23.83	0.044	0.479
2-propanol	0.9972	0.01	2.19	0.009	0.054	0.9992	0.11	22.57	0.048	0.305	0.9979	-0.02	24.13	0.079	0.527
benzene	0.9996	0.02	7.92	0.013	0.072	0.9963	0.13	69.49	0.358	2.006	0.9967	-0.07	20.59	0.342	0.561
dichloromethane	0.9993	0.13	16.60	0.073	0.255	0.9991	0.50	91.89	0.464	1.615	0.9986	-0.20	12.97	0.591	0.284
chloroform	0.9985	0.22	39.47	0.182	0.879	0.9975	1.34	210.58	1.260	6.096	0.9991	0.16	12.52	0.758	0.213
hexafluorobenzene	0.9979	0.11	6.91	0.034	0.185	0.9997	0.25	24.76	0.047	0.259	0.9968	-0.12	8.37	0.157	0.272
dibromomethane	0.9985	0.38	45.18	0.179	1.028	0.9975	0.47	143.09	0.726	4.176	0.9985	-0.73	7.43	0.586	0.168
bromoform	0.9989	0.23	55.20	0.179	1.069	0.9992	0.40	155.11	0.420	2.510	0.9998	-0.24	6.59	0.235	0.058

PEO clear film	Δf^*_{max} vs P/P°					$\Delta h_{\text{max}}/h_b$ vs P/P°					$\Delta h_{\text{max}}/h_b$ vs Δf^*_{max}				
	R^2	intcpt	slp	intcpt err	slp err	R^2	intcpt	slp	intcpt err	slp err	R^2	intcpt	slp	intcpt err	slp err
hexane	0.9975	0.00	0.60	0.006	0.014	0.9922	0.00	0.26	0.004	0.011	0.9945	0.00	1.01	0.004	0.036
2-propanol	0.9986	0.01	2.12	0.012	0.040	0.9980	0.02	0.92	0.006	0.020	0.9989	0.01	1.01	0.004	0.017
benzene	0.9966	0.05	5.72	0.021	0.167	0.9929	0.03	2.41	0.013	0.102	0.9963	0.01	0.99	0.010	0.030
dichloromethane	0.9916	0.05	14.55	0.094	0.600	0.9892	0.04	3.88	0.028	0.182	0.9970	0.02	0.63	0.015	0.015
chloroform	0.9975	0.04	38.52	0.052	0.789	0.9957	0.02	9.94	0.018	0.267	0.9983	0.01	0.61	0.011	0.010
hexafluorobenzene	0.9986	-0.01	2.05	0.016	0.031	0.9981	0.00	0.39	0.003	0.007	0.9989	0.01	0.44	0.003	0.006
dibromomethane	0.9978	0.13	40.44	0.062	0.742	0.9974	0.03	7.48	0.013	0.150	0.9985	0.00	0.43	0.010	0.006
bromoform	0.9905	0.06	51.26	0.139	1.972	0.9905	0.01	8.61	0.023	0.331	0.9986	0.00	0.39	0.009	0.006

^a Mass-normalized maximum resonant frequency change, Δf^*_{max} , vs the fraction of the analyte's vapor pressure (Δf^*_{max} vs P/P°), relative differential resistance increase vs the fraction of the analyte's vapor pressure ($\Delta R_{\text{max}}/R_b$ vs P/P°), relative differential thickness increase vs the fraction of the analyte's vapor pressure ($\Delta h_{\text{max}}/h_b$ vs P/P°), relative differential resistance increase vs mass-normalized maximum resonant frequency change ($\Delta R_{\text{max}}/R_b$ vs Δf^*_{max}), and relative differential thickness increase vs mass-normalized maximum resonant frequency change ($\Delta h_{\text{max}}/h_b$ vs Δf^*_{max}) are tabulated.

EXPERIMENTAL SECTION

QCM crystals (10 MHz, blank diameter = 13.7 mm) with a custom electrode pattern were obtained from International Crystal Manufacturing (ICM), Oklahoma City, OK. The standard oscillation electrodes were configured at 90° angles to make room for two other tabs that would serve as electrodes for resistance measurements of the carbon black–polymer composite films (Figure 1). The crystals were polished to a surface roughness of less than 5 μm , which produced a mirrorlike finish on the gold electrodes. To facilitate reflection of the ellipsometer's laser beam when the crystals were used with transparent films during the thickness measurements, one oscillator electrode was larger than the other (larger electrode diameter = 7.8 mm, smaller electrode

diameter = 5.1 mm). The resistance tabs were not used during the thickness vs QCM frequency measurements on films that were not filled with carbon black. Similarly, the ellipsometer was not used during the resistance vs QCM frequency measurements in which optically opaque, carbon-black-filled, composite films were used.

The vapor stream was produced by passing general laboratory compressed air through analyte solvents contained in custom bubblers. The solvents were of HPLC quality (Aldrich Chemical Co.) and were used as received. Saturation of the vapor with solvent was confirmed by mass loss experiments.⁹ The solvent-saturated air was then diluted to the desired concentration with house air. The air flows through the bubbler and in the back-

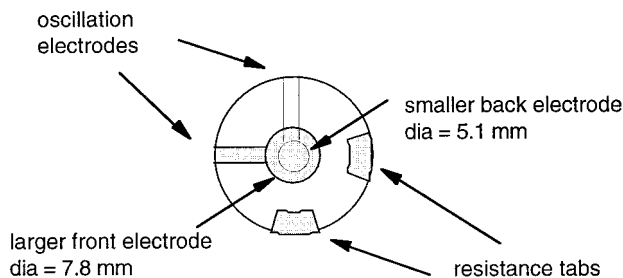


Figure 1. Custom 10 MHz quartz crystal microbalance with oscillation electrodes and tabs for reading the resistance of the composite film. Shaded areas indicate regions coated with Au. The larger electrode was used to facilitate ellipsometry measurements.

ground gas were regulated by needle valves, and the flows in both streams were monitored with Gilmont rotameters (VWR Scientific). The concentration of analyte in the vapor stream was independently verified using a calibrated flame ionization detector (California Analytical, Santa Ana, CA).

Two polymers were used in this work, poly(caprolactone) (PCL) and poly(ethylene oxide) (PEO). Films of these polymers that contained carbon black were used for the resistance measurements, while transparent, pure polymer films were used for the thickness measurements. All films were cast from standard solutions that consisted of 160 mg of polymer dissolved in 20 mL of benzene to which 40 mg of carbon black was added to make composite films (resulting in solutions that were 20 wt % carbon black). All solutions were sonicated for at least 5 min immediately prior to casting the films. The polymer films were spun-cast on a spin coater (Headway Research, Garland, TX) at 2000 rpm, and the average film thickness was obtained by profilometry (Dektak 3030, Sloan Technology Corp., Santa Barbara, CA).

The QCM crystals were weighed before and after film application using a Cahn microbalance (resolution 0.001 mg; Cahn C-35, Orion Research, Beverly, MA) to obtain the masses of the films that were deposited over the active electrode (5.1 mm diameter area) of the QCM. The PCL clear film mass was $40 \mu\text{g cm}^{-2}$ and 375 nm thick, while the PCL-carbon black composite film mass was $185 \mu\text{g cm}^{-2}$ with a baseline resistance of $\approx 12 \text{ k}\Omega$. The PEO clear film had a mass of $120 \mu\text{g cm}^{-2}$ and a thickness of 1090 nm, while the PEO-carbon black composite film was $19 \mu\text{g cm}^{-2}$ with a baseline resistance of $\approx 16 \text{ k}\Omega$. Using the clear polymer film areas and the mass and thickness values above, densities for the clear films of PEO and PCL were calculated and agreed with literature values for these polymers.

Resistances were measured using a 2002 digital multimeter (Keithley, Cleveland, OH), and the resonant frequency of the QCM was obtained using a 5384A frequency counter (Hewlett-Packard, Palo Alto, CA). Ellipsometry measurements were taken on an L116C ellipsometer (Gaertner Scientific, Chicago, IL). Optical constants were obtained for each surface before the films were applied. The index of refraction of each polymer film was taken from the literature. The absorption coefficient for the film was obtained using the two-angle technique,^{10,11} which also provided an independent measurement of the index of refraction

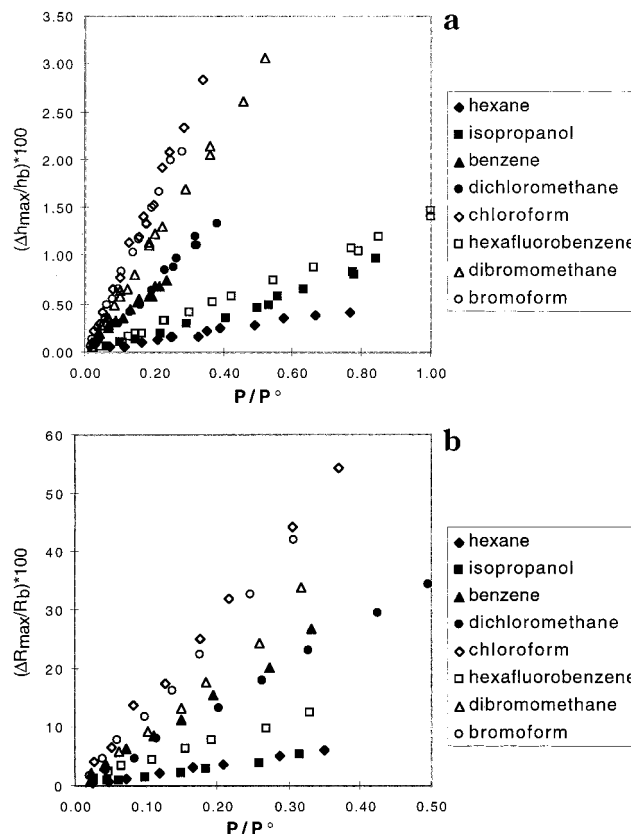


Figure 2. (a) Relative differential thickness increase for a pure PCL film vs fraction of analyte vapor pressure exposed to the film. (b) Differential relative resistance increase in a PCL-carbon black composite vs fraction of analyte vapor pressure exposed to the film.

and thickness of the film. The film thicknesses obtained by ellipsometry agreed to within 10% with the values obtained by profilometry.

To initiate an experiment, a baseline value was recorded for the QCM resonant frequency, resistance, and/or thickness of the film. The film was then exposed to analyte vapor until steady-state values were reached as determined by constant output readings from the instruments. The data were recorded manually for convenience. Thickness measurements were taken three to five times after steady state had been reached for a given vapor, and the average result was recorded for both the baseline and the steady-state, solvent-exposed values.

RESULTS

Figure 2a shows the relative thickness change, $\Delta h_{\text{max}}/h_b$, where Δh_{max} is the thickness change of the film during exposure to the analyte vapor and h_b is the baseline thickness of the film in air prior to analyte exposure, of poly(caprolactone) films as a function of the fraction of the analyte's vapor pressure, P/P° . The series of test vapors used in these experiments is representative of a broad test set of analytes that have been used previously to investigate the discrimination ability of arrays of conducting polymer composite vapor detectors.¹⁻³ The data of Figure 2a are well-fit to a linear dependence of $\Delta h_{\text{max}}/h_b$ on P/P° (Table 1). Figure 3a shows similar data for poly(ethylene oxide) films.

Figures 2b and 3b depict the steady-state relative differential resistance responses, $\Delta R_{\text{max}}/R_b$, where ΔR_{max} is the resistance

(9) Atkins, P. W. *Physical Chemistry*; W. H. Freeman and Co.: New York, 1994.
 (10) Comfort, J. C.; Urban, F. K.; Barton, D. *Thin Solid Films* **1996**, 291, 51.
 (11) Urban, F. K. *Appl. Surf. Sci.* **1988**, 33, 934.

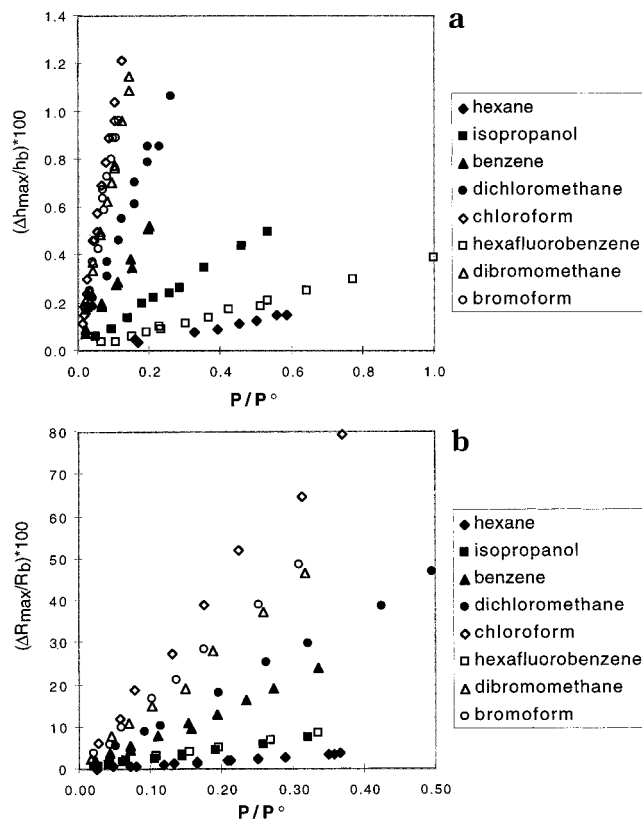


Figure 3. (a) Relative differential thickness increase for a pure PEO film vs fraction of analyte vapor pressure exposed to the film. (b) Differential relative resistance increase in a PEO–carbon black composite vs fraction of analyte vapor pressure exposed to the film.

change of the film during exposure to the analyte vapor and R_b is the baseline resistance of the film in air prior to analyte exposure, of carbon-black filled poly(caprolactone) and poly(ethylene oxide) films, respectively, as a function of the analyte concentration, for the same set of test analytes. Over the concentration ranges probed in the experiment, the data are well-fit by straight lines passing through the origin (Table 1).

Figure 4 depicts the mass-normalized maximum resonant frequency change, Δf^*_{\max} , of the poly(caprolactone) films on a QCM crystal during exposure to the analyte vapor. The frequency shifts were all negative upon sorption of analyte, and only absolute values of Δf are reported herein. The observed resonant frequency change was normalized by the mass of the films (as determined by the Cahn microbalance measurements) in the active QCM area to remove any variability due to the use of different film thicknesses and/or film masses between experiments on a given type of polymer. Figure 5 depicts the same data for poly(ethylene oxide) films. Data are depicted for films of polymer that were and were not, respectively, filled with carbon black. Again the data are well-fit by straight lines over the analyte concentration range of experimental interest (Table 1). For all the solvents, the Δf^*_{\max} value of a pure polymer film was the same as the Δf^*_{\max} value of the analogous carbon-black-filled composite to within the error in the measurements. For example, Figure 6 depicts the Δf^*_{\max} value as a function of P/P° for CHCl_3 sorbed in poly(caprolactone)– and poly(ethylene oxide)–carbon black composites and in pure polymer films without carbon black added.

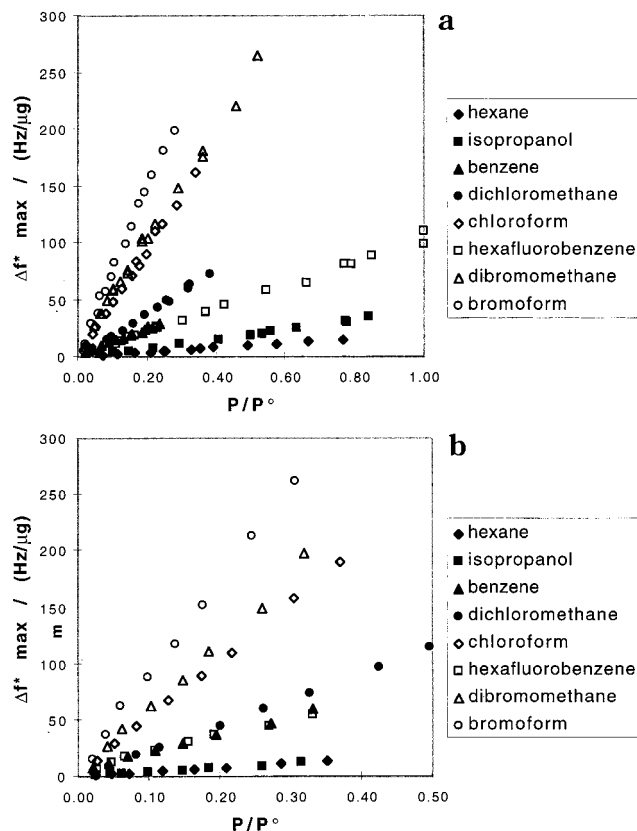


Figure 4. Mass-normalized maximum resonant frequency change vs fraction of analyte vapor pressure exposed to the film for (a) a PCL film without carbon black and (b) a PCL–carbon black composite.

DISCUSSION

Figure 7a depicts a plot of the relative differential dc resistance change of the poly(caprolactone) film, from electrical measurements, as a function of the fractional swelling of the polymer, as determined by optical ellipsometry measurements. The same analysis for a second poly(caprolactone) film is shown in Figure 7b to illustrate the variance in the data. For both polymer systems, the slopes and intercepts of the $\Delta R_{\max}/R_b$ vs P/P° data for the composite films were used to predict what values of $\Delta R_{\max}/R_b$ would be expected for the P/P° values used in the measurements for the nonfilled polymer films. Likewise, the slopes and intercepts of the $\Delta h_{\max}/h_b$ vs P/P° data for the nonfilled polymer films were used to predict what values of $\Delta h_{\max}/h_b$ would be expected for the P/P° values used in the measurements for the composite films. The predicted values of $\Delta R_{\max}/R_b$ were then plotted vs the predicted $\Delta h_{\max}/h_b$ values at the corresponding P/P° values of the analytes. As displayed in Figure 7, the data are linear and roughly fall on the same line for all of the test vapors investigated in this work. For each film, some solvents do not lie on the common line, but this is presumed to be due to experimental error in the delivery of the vapor.¹² A robust interpretation of the relatively small deviations of the behaviors of the various analytes on a given polymer film vs the common line would require implementation of methods that could determine the resistance and thickness changes simultaneously on one detector, and such methods were not available in this study. The data of Figure 7 clearly indicate that, regardless of the analyte used, a given

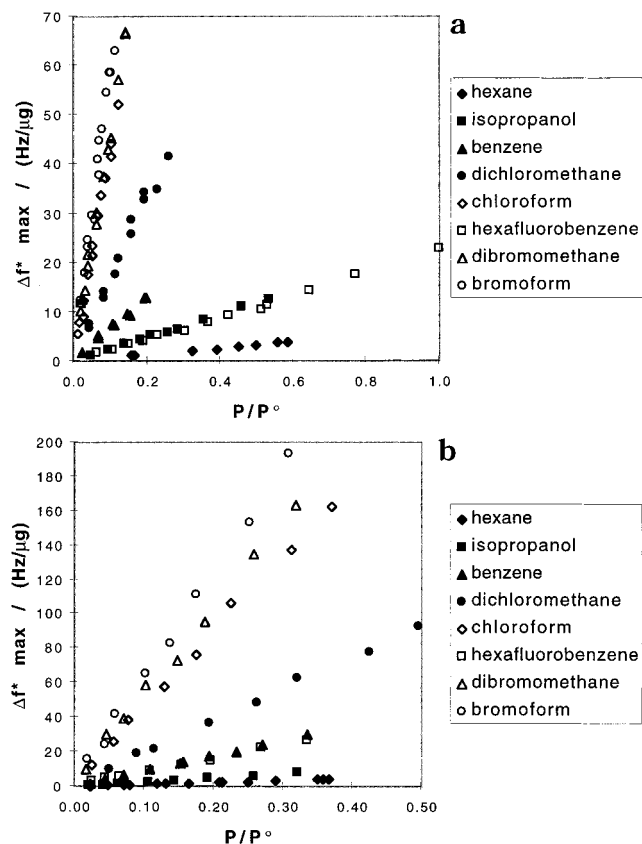


Figure 5. Mass-normalized maximum resonant frequency change vs fraction of analyte vapor pressure exposed to the film for (a) a PEO film without carbon black and (b) a PEO-carbon black composite.

fractional thickness change of the polymer produces a given steady-state relative differential resistance response of the corresponding carbon-filled composite, at least for the polymer-analyte combinations explored in this work. Thus, the hypothesis of concern—that volumetric film swelling is the key variable determining $\Delta R_{\max}/R_0$ in the composite carbon black-insulating polymer detectors—seems to be confirmed from the data obtained in this work, at least for the analytes and polymers investigated to date. Also, these data indicate that the relationship between relative thickness change and steady-state relative differential resistance change is linear, at least over the range of analyte concentrations investigated in this work.

One complicating factor is that the thickness measurements obtained in this work were performed on pure polymeric materials, while the $\Delta R_{\max}/R_0$ measurements were performed on carbon-black-filled polymer composites. The assumption made above in interpreting the data of Figure 7 is that the volumetric swellings of the polymers are similar whether or not the material is filled with carbon black. Given the linear relationship deduced between

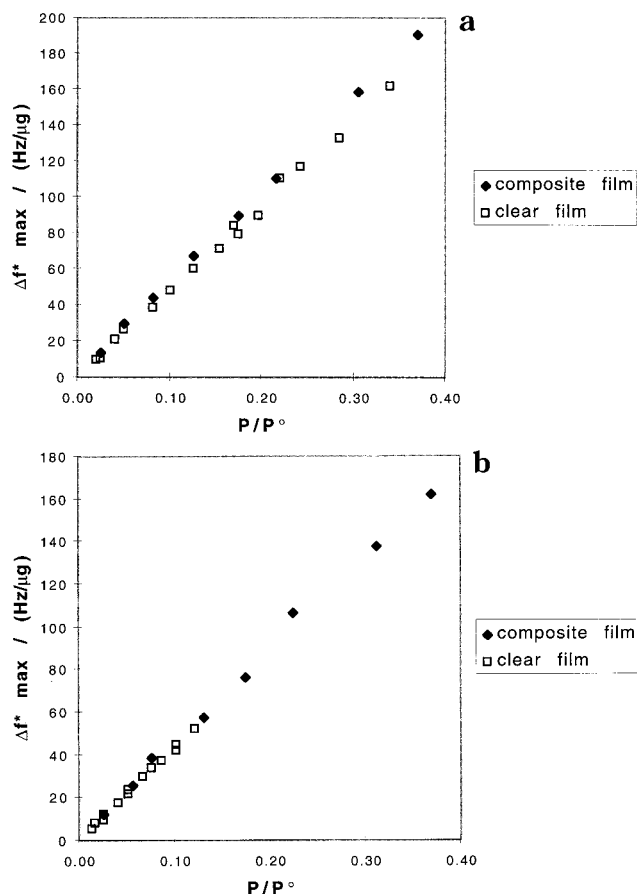


Figure 6. Mass-normalized maximum resonant frequency change vs fraction of analyte vapor pressure exposed to the film for (a) PCL-carbon black composites and PCL films without carbon black and (b) PEO-carbon black composites and PEO films without carbon black.

$\Delta h_{\max}/h_0$ and $\Delta R_{\max}/R_0$ and the low likelihood that, over a range of analytes and concentrations, two separate functional dependencies of swelling on analyte concentration would precisely counteract each other to yield the data of Figure 7, this assumption seems quite reasonable. Given the linear dependence of $\Delta R_{\max}/R_0$ on P/P° that has been observed for other test analytes,¹³ it seems reasonable to assume that the relationship between relative volumetric swelling and relative differential resistance measurements is extendible, at least to first order, for those composite-analyte combinations as well.

An independent check on the validity of the relationship between swelling in the carbon-black-filled composites and the pure polymer films is available from the QCM resonant frequency measurements. The relationship between $\Delta R_{\max}/R_0$ vs Δf_{\max}^* and $\Delta h_{\max}/h_0$ vs Δf_{\max}^* is linear as seen in Figure 8 for PCL and in Figure 9 for PEO (see also Table 1). The slopes and intercepts of the $\Delta R_{\max}/R_0$ vs Δf_{\max}^* data for the composite films were used to predict what values of $\Delta R_{\max}/R_0$ would be expected for the Δf_{\max}^* values measured for the nonfilled polymer films at the various analyte concentrations used in the measurements. Likewise, the slopes and intercepts of the $\Delta h_{\max}/h_0$ vs Δf_{\max}^* data for the nonfilled polymer films were used to predict what values of

(12) The relationship between the resistance change and the volume swelling depends on the carbon-black loading and other parameters involved in making the films. Under controlled conditions where several films are made in a single batch process from a single carbon black-polymer suspension, the variability in response between films to a given analyte concentration is typically less than 10%. The higher variability between the two films of Figure 7 results from the fact that they were made on two separate occasions with no attempt to control fully the deposition process or the suspension properties for consistency between batches.

(13) Severin, E. J.; Doleman, B. J.; Lewis, N. S. *Anal. Chem.* **2000**, *72*, 658-668.

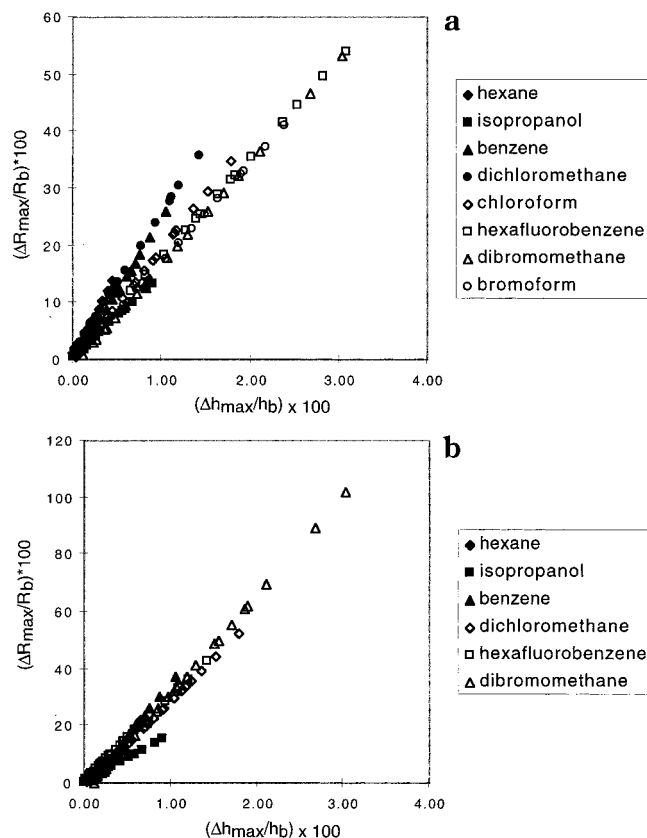


Figure 7. Relative differential resistance increase for a PCL-carbon black composite film vs relative differential thickness increase for a PCL clear film when both films were exposed to various analytes at various fractional vapor pressures, correlated by the analyte fractional vapor pressure for two separate (a, b) PCL films.

$\Delta h_{\max}/h_b$ would be expected for the Δf_{\max}^* values measured for the composite films at the various analyte concentrations used in the measurements. The predicted values of $\Delta R_{\max}/R_b$ were then plotted vs the predicted $\Delta h_{\max}/h_b$ values at the corresponding P/P° values of the analytes. As displayed in Figure 10, the data for each solvent are linear and roughly fall on the same line for all of the test vapors investigated in this work. This strongly implies the presence of a correlation between volume change and resistance change in these composite films. This is a stronger indicator than the correlation using P/P° because the Δf_{\max}^* value for each presentation for each film was taken simultaneously with the $\Delta R_{\max}/R_b$ and $\Delta h_{\max}/h_b$ measurements. The correlation calculated from P/P° presented above was less precise because of variance in the flow system, whereas any changes in the concentration of the exposed analyte would be reflected in the Δf_{\max}^* value as well.

In our work, the frequency shift of the polymer-coated QCM crystals arising from sorption of the analyte vapor was <2% of the resonant frequency of the polymer-coated crystal. Under such conditions, prior work has concluded that mechanical losses are minimal and that the frequency shifts are predominantly due to changes in mass uptake.^{8a} Although under such conditions the frequency shifts observed in the QCM data can be related, through the proportionality between Δf_{\max} and Δm_{\max} implied by the Sauerbrey equation,^{8a,b} to the fractional mass uptake of these films, the validity of this relationship is not necessary to support any of the key conclusions of our study. Regardless of the physical

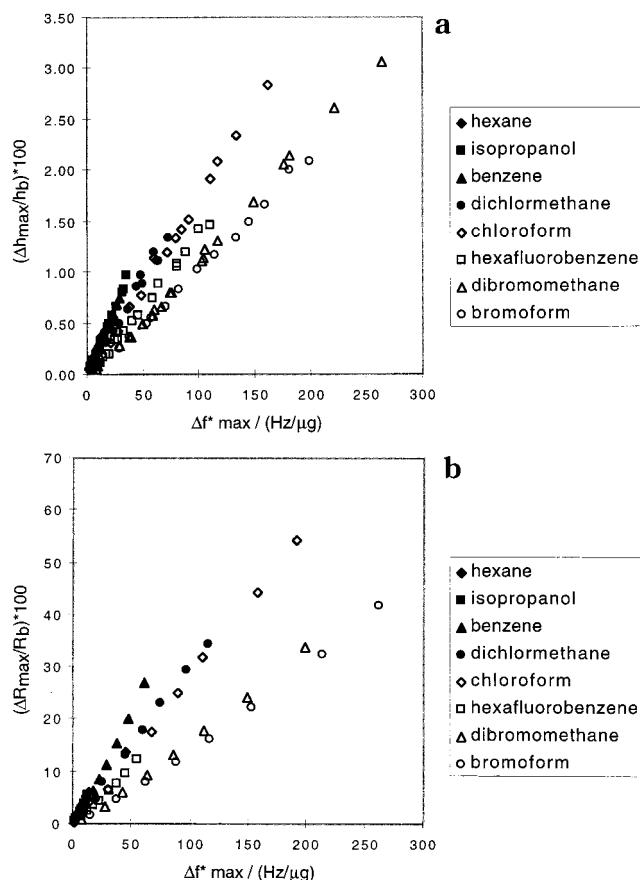


Figure 8. (a) Relative differential thickness increase vs mass-normalized maximum resonant frequency change for a PCL film exposed to various analyte pressures. (b) Relative differential resistance increase vs mass-normalized maximum resonant frequency change for a PCL film exposed to various analyte pressures.

phenomena that produce a shift in the resonant frequency of the polymer-coated QCM crystals upon vapor sorption, it is clear that the key variable correlating with the $\Delta R_{\max}/R_b$ responses of various analytes for a given type of polymer is not Δf_{\max} , Δf_{\max}^* , or $\Delta m_{\max}/m_b$ (with Δm_{\max} deduced from Δf_{\max} through the Sauerbrey equation) but instead that the experimentally observed correlation is with $\Delta h_{\max}/h_b$.

Further support for the swelling-induced resistance change hypothesis can be obtained by investigating the relationship between $\Delta R_{\max}/R_b$ and $\Delta h_{\max}/h_b$ as a function of analyte density. As seen in Figures 11 and 12, the slopes of the $\Delta h_{\max}/h_b$ vs Δf_{\max}^* lines and the $\Delta R_{\max}/R_b$ vs Δf_{\max}^* lines depend linearly on the density (as measured in the pure liquid phase) of the sorbing species. These data are in agreement with recently reported results that were obtained in parallel with our study, in which the relative differential resistance response of carbon-black-filled poly(ethylene oxide) composites was shown to correlate with the density of the gaseous analyte (as measured in its pure liquid phase).¹⁴

These data support the hypothesis that the resistance response is primarily induced by a change in the volume of the film as reflected in the thickness change. A straight line of any slope for $[\Delta f_{\max}^*/(\Delta R_{\max}/R_b)]$ vs density that goes through the origin

(14) Swann, M. J.; Glidle, A.; Cui, L.; Barker, J. R.; Cooper, J. M. *Chem. Commun.* **1998**, 2753–2754.

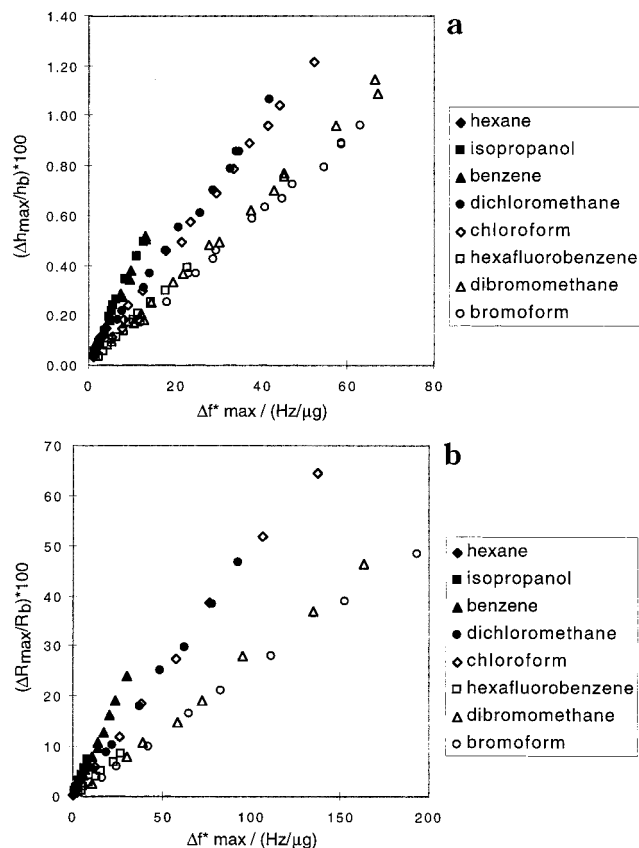


Figure 9. (a) Relative differential thickness increase vs mass-normalized maximum resonant frequency change for a PEO film exposed to various analyte fractional vapor pressures. (b) Differential relative resistance increase vs mass-normalized maximum resonant frequency change for a PEO film exposed to various analyte fractional vapor pressures.

would imply a precise correlation between the density and the detector response. The $[\Delta f^*_{\max}/(\Delta R_{\max}/R_b)]$ ratio for hexafluorobenzene is larger in all cases, most likely because the molecules do not chemisorb into the polymer matrix in proportion to the amount that physisorbs because molecular interactions between the perfluorinated analyte and the polymer chains are not likely to be sufficiently favorable energetically to disrupt the polymer interchain interactions. This would cause an increase in QCM resonant frequency response for hexafluorobenzene (due to adsorption) without a concomitant increase in resistance or thickness response (which requires absorption), leading to larger $[\Delta f^*_{\max}/(\Delta R_{\max}/R_b)]$ and $[\Delta f^*_{\max}/(\Delta h_{\max}/h_b)]$ ratios for that solvent.

Generally, the slope of the line for the thickness response vs the density is about an order of magnitude larger than the slope of the line for the related resistance response measurements. In both the thickness and resistance measurements the Δf^*_{\max} responses are similar; therefore, the difference in slopes is due to differences in relative response between the thickness and resistance measurements. In all cases, the relative differential resistance response is greater than the relative thickness change for a given Δf^*_{\max} change. This finding is consistent with percolation theory, which relates the fractional volume change of a conductor in a composite to a fractional resistivity change of that composite for a given initial conductor volume fraction. We

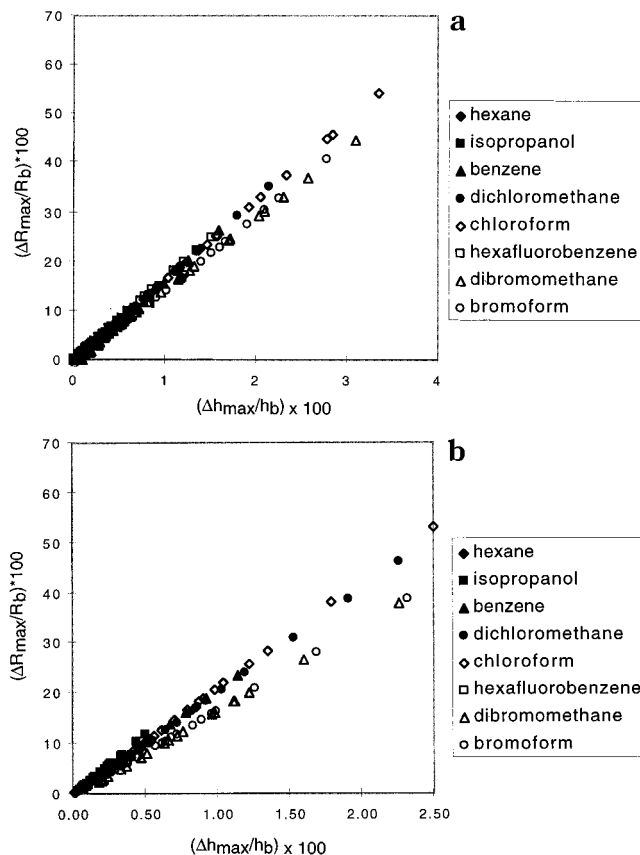


Figure 10. Relative differential resistance increase for a polymer-carbon black composite film vs relative differential thickness increase for a polymer clear film when both films were exposed to various analytes at various pressures, correlated by the mass-normalized maximum QCM resonant frequency change in each film recorded during those analyte exposures for (a) PCL and (b) PEO films.

are unable to make direct comparisons with percolation theory because we do not have a complete understanding of the morphology of the carbon black in the composites; however, these data are consistent with reasonable values for the variables in the percolation theory equation for high-conductivity carbon black.^{15–17}

An implication of these findings is that low-density analytes will cause a larger resistance response in our detectors for a given Δf^*_{\max} value. We have shown in prior work that the amount of analyte that sorbs into these detector films is a function of the fraction of vapor pressure of the analyte.¹⁸ This P/P° dependence accounts for most of the response by a detector to an analyte, but the differences in response by a detector to a set of analytes are due to differences in chemical affinity between the polymer film and the analytes as well as the molecular properties of the analytes such as their molecular volume. Therefore, at the same level of sorption (mass uptake), a lower density analyte will be easier to detect than a higher density analyte.

In conclusion, we have shown that the composite detectors respond according to the volume change of the composite film

- (15) Ali, M. H.; AboHashem, A. *J. Mater. Process. Technol.* **1997**, *68*, 163.
- (16) Ali, M. H.; AboHashem, A. *J. Mater. Process. Technol.* **1997**, *68*, 168.
- (17) Ali, M. H.; AboHashem, A. *Plast. Rubber Compos. Process. Appl.* **1995**, *24*, 47.
- (18) Doleman, B. J.; Severin, E. J.; Lewis, N. S. *Proc. Natl. Acad. Sci. U.S.A.* **1998**, *95*, 5442–5447.

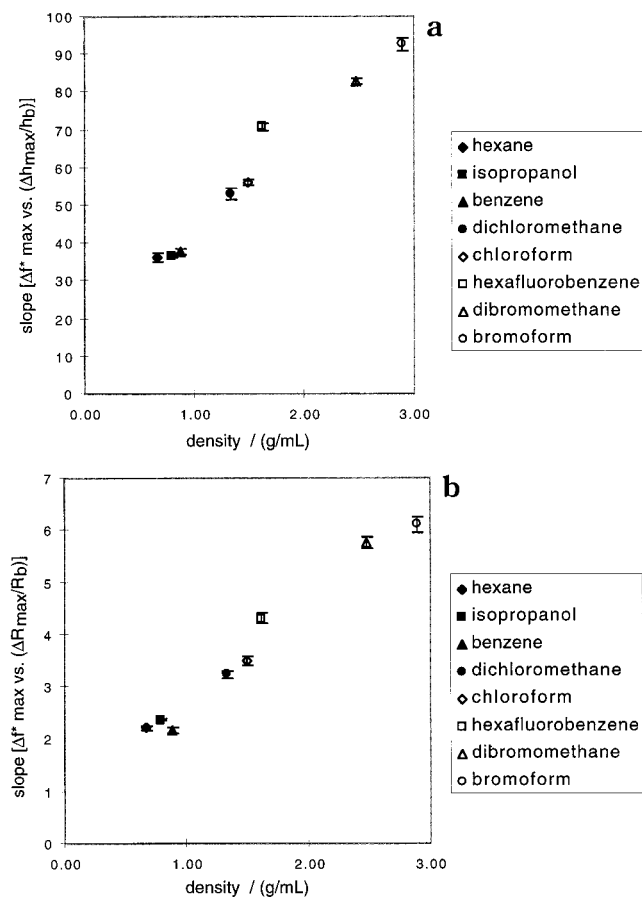


Figure 11. (a) Value of the slope of the line corresponding to [$\Delta f^*_{\text{max}}/(\Delta h_{\text{max}}/h_b)$] for a clear PCL film for various analyte presentations at various analyte fractional vapor pressures vs the analyte liquid-phase density for the exposed analyte. (b) Value of the slope of the line corresponding to [$\Delta f^*_{\text{max}}/(\Delta R_{\text{max}}/R_b)$] for a PCL–carbon black composite film for various analyte presentations at various analyte fractional vapor pressures vs the analyte liquid-phase density for the exposed analyte.

as evidenced by a linear dependence on the analyte densities of the slopes of the lines for the thickness and resistance responses vs film-coated QCM resonant frequency change and by a linear relationship between percent resistance change and percent thickness change when these two are correlated by the film-coated QCM resonant frequency changes. Additionally, we have developed a single-element densitometer that can be used to character-

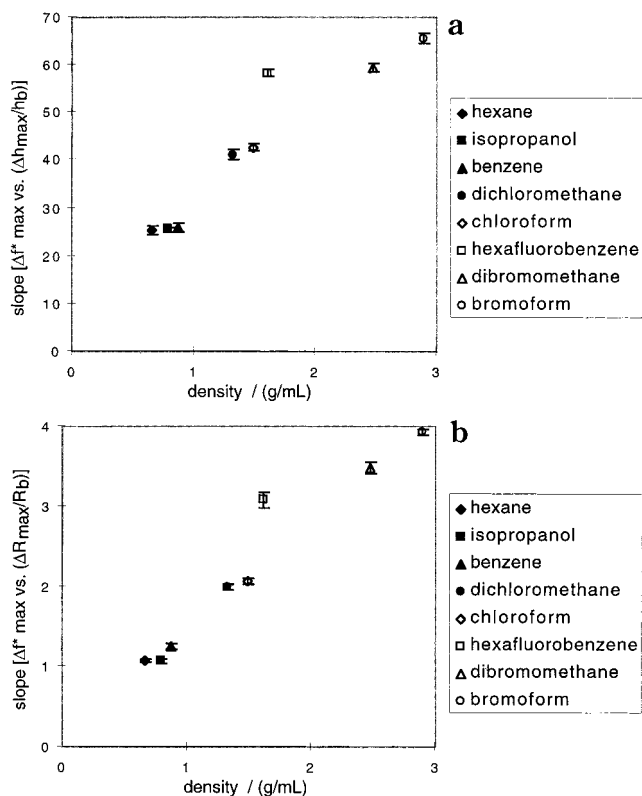


Figure 12. (a) Value of the slope of the line corresponding to [$\Delta f^*_{\text{max}}/(\Delta h_{\text{max}}/h_b)$] for a clear PEO film for various analyte presentations at various analyte pressures vs the analyte liquid-phase density for the exposed analyte. (b) Value of the slope of the line corresponding to [$\Delta f^*_{\text{max}}/(\Delta R_{\text{max}}/R_b)$] for a PEO–carbon black composite film for various analyte presentations at various analyte pressures vs the analyte liquid-phase density of the exposed analyte.

ize in a convenient manner a molecular property of many different types of analytes presented to these types of detectors.

ACKNOWLEDGMENT

This work was supported by the National Aeronautics and Space Administration, the Army Research Office, and the Defense Advanced Research Projects Agency.

Received for review September 7, 1999. Accepted January 11, 2000.

AC991026F